Chapter 10
Civil Aircraft Vehicle Design

A. Sgueglia, S. Dubreuil (✉), and N. Bartoli
e-mail: sylvain.dubreuil@onera.fr

10.1 Introduction

In the recent years, aviation is facing with the increasing of fuel price and flights, and the impact is estimated to grow more and more in next years without any action (Collier and Wahls 2016). To reduce its environmental footprint, engineers are trying to design more efficient aircraft, with engines less consuming. However, the classical aircraft's tube and wing configuration has been developed over half a century, and it still offers small potential gain. A breakthrough in aircraft design is then needed to drastically reduce the problem. Innovation can be brought at aircraft's configuration level (considering different architecture than the tube and wing, like the Blended Wing Body (Liebeck 2004; Sgueglia et al. 2018b), see Chapter 11 for an example of Blended Wing Body design problem) or at propulsive level, introducing a partial or total electrification in the propulsive chain (Friedrich and Robertson 2015). In any case, the problem of designing an unconventional aircraft is more complex than the classical one, due to the strong coupling between disciplines, as shown by different authors, for instance by Brelje and Martins (2018). For example, in an electric architecture, thermal aspects play a key role due to the power dissipated by electrical components, or the distributed propulsion fans change the flux on the wing, and the overall aerodynamics performance is then modified (aeropropulsive effects). This chapter presents an unconventional large passenger aircraft, with a hybrid distributed propulsion, considering an entry into service (EIS) in 2035. The concept has been proposed by Sgueglia et al. (2018a). The aircraft is designed thanks to FAST (Fixed−wing Aircraft Sizing Tool, (Schmollgruber et al. 2017)), a multidisciplinary code that takes into account all key disciplines and interactions between them. Since we are dealing with EIS2035, hypotheses on the technological level for that horizon are formulated. In the literature, there are multiple assumptions, an uncertainty-based study is presented here to cover all the possible values in the 2035 perspectives. Multidisciplinary analysis formulations

L. Brevault et al., *Aerospace System Analysis and Optimization in Uncertainty*,
Springer Optimization and Its Applications 156,
https://doi.org/10.1007/978-3-030-39126-3_10

are compared, to understand how the technology impacts the design, comparing a case in which the geometry is fixed and another one in which geometry is being resized, to ensure some design constraints.

The chapter is organized as follows: Section 10.2 presents the concept of hybrid electric aircraft. Section 10.3 describes the propulsion chain architecture and Section 10.4 presents the design tool used for the study. Finally, in Sections 10.5 and 10.6 are described the sensitivity analysis using Sobol indices calculated using Polynomial Chaos Expansion and the obtained results.

10.2 Hybrid Electric Aircraft Concept

For the concept proposed in this chapter, the following features are requirements to match the aviation's goals for next years (Sgueglia et al. 2018a):

- Hybrid electric (HE) propulsive architecture,
- capability to fly with zero emission up to 3000 ft (about 1 km), that corresponds to atmospheric boundary layer height, in which convective phenomena are relevant. This is the most critical zone, in which harmful molecules are mixed, with negative results on human beings,
- entry into service in 2035,
- performance in terms of fuel consumption not worse than a conventional aircraft, with the same 2035 hypotheses.

The hybrid electric chain is integrated within a distributed propulsion architecture, that allows to have advantages in terms of take−off field length, de-sizing of wing surface, and reduction of engines' weight (Kirner 2015). The aircraft definitive concept is shown in Figure 10.1.

The propulsive chain is made up of different components:

- turbogenerators, which are the ensemble of a fuel burning engine and a converter device (to convert mechanical power into electrical power),
- batteries (not shown in Figure 10.1) to provide electric power, located in the cargo hold,
- electric motors and ducted fans, distributed at wing upper surface trailing edge,
- DC/DC and DC/AC converter (called, respectively, converter and inverter) in order to switch from alternate and direct current for transportation and utilisation and at the same voltage,
- cables for the current transport, including safety reinforcement,
- cooling system to dissipate heat generated by power losses.

Regarding the energy source positions, turbogenerators are at the rear to reduce pylons wetted area and interferences with the wing. Thus, the only possible choice for the empennage is a T-tail architecture. Batteries are instead located in the cargo

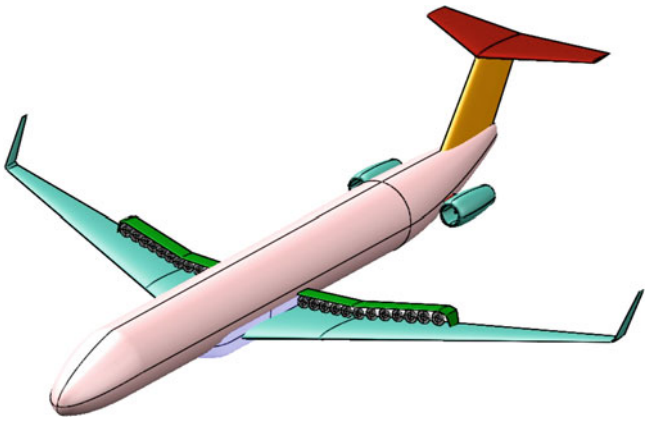

Fig. 10.1 Hybrid aircraft concept proposed with distributed electric ducted fan (Sgueglia et al. 2018a)

freight; the choice has been dictated primarily for the volumetric space needed, and also because they introduce a non negligible weight. Having them around the wing reduces their impact on the stability, since they are in proximity of the center of gravity. The main drawback of this disposition is that some cargo volume is not available anymore for luggages, thus the maximum payload is reduced.

10.3 Propulsive Chain Architecture

Energy sources and electrical components are connected as in Figure 10.2, which shows the generic propulsive schema. Batteries and generators are connected through an electrical node (bus); converters and inverters are placed to convert mechanical power into electrical power and bring the current at the right transport voltage. Power management is obtained through two different power rates, one for each energy source (δ_b for the battery and δ_g for the turbogenerator):

$$\delta_b = \frac{P_b}{P_{b,\max}} \tag{10.1a}$$

$$\delta_g = \frac{P_g}{P_{g,\max}} \tag{10.1b}$$

where P_b and P_g identify the power demanded by batteries and generators, respectively, and the subscript max indicates the maximum delivered power. This approach allows flexibility, mainly to deal with failure cases (Sgueglia et al. 2018a). Thus, the total power at the electrical node is

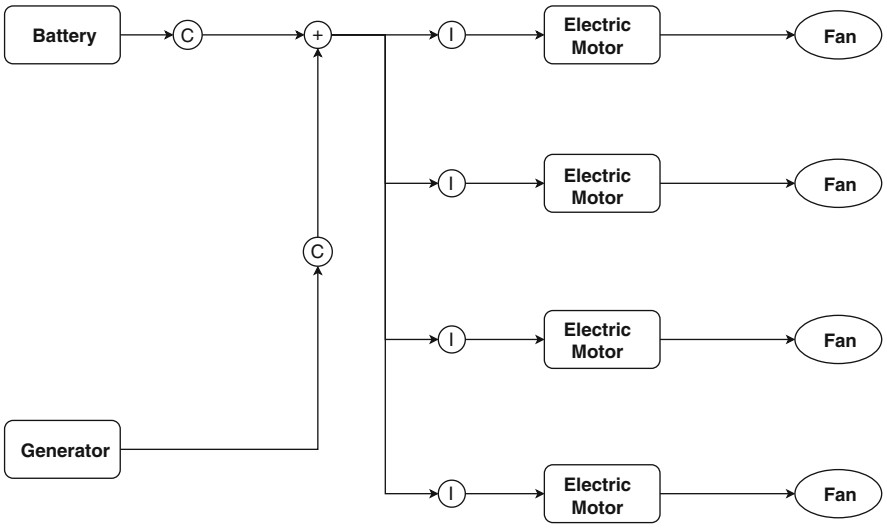

Fig. 10.2 Distributed electric propulsion architecture (Sgueglia et al. 2018a)

$$P_{tot} = \eta_b \delta_b P_{b,\max} + \eta_g \delta_g P_{g,\max} \tag{10.2}$$

in which η represents efficiency. Up to the electrical node, the architecture is a serial one. Then, power is splitted to all the fans:

$$P_{fan} = \frac{1}{N} P_{tot} \eta_{em} \eta_i \tag{10.3}$$

with P_{fan} the power delivered to fan, N the number of engines, and η_{em} and η_i the efficiencies of motors and inverters. In the scheme power rates can be inputs to obtain total thrust (left to right direction), or thrust can be an input and the required power rates coherent with needed thrust outputs (from right to left). However, it may also be eliminated since it does not add anything to the rest of the explanation The power required by the secondary systems (control system, ice protection devices, lighting, and so on) is loaded on batteries. Estimation of this power is found in the work of Seresinhe and Lawson (2014) for a more electric aircraft A320 type.

At the preliminary design level, low computational cost is a requisite to obtain results in a reasonable time, thus propulsive and electrical components are modeled with low fidelity methods, described in next sections.

10.3.1 Battery Model

Battery is a vital component as it is a main source of power as it introduces significant weight to the entire system (Lowry and Larminie 2012; Tremblay and Dessaint 2009). Research recently focuses on developing newer and more efficient batteries (such as the lithium air, lithium sulfur batteries, or even integrated concepts), but the work is still at the early stage, thus their performances are hardly predictable; for this reason in the concept here studied a classical Li-Ion battery type is preferred. Also, for each battery's type, multiple choices are possible, according to the required performances: in general, more powerful a battery is, less energy can be stored in it. For large passenger aircraft, both power and energy are relevant, thus a compromise between the two has to be found. In conclusion, the battery's choice is never an easy task and depends on the overall design.

Five parameters fully define a battery, as reported in Tremblay and Dessaint (2009):

- specific energy density e_b, that is the energy stored per unit mass,
- energy density $\rho_{E,b}$, that is the energy stored per unit volume,
- specific power density p_b, that is the power delivered per unit mass,
- power density $\rho_{P,b}$, that is the power delivered per unit volume,
- density ρ_b, that is the mass per unit volume.

These variables are not independent of each other, but only three of them are necessary. The model here adopted takes specific energy and power as inputs; volumetric densities are then computed as:

$$\rho_{E,b} = \rho_b e_b \tag{10.4a}$$

$$\rho_{P,b} = \rho_b p_b \tag{10.4b}$$

and the battery's parameters are finally deduced:

$$m_b = \rho_b \tau_b \tag{10.5a}$$

$$E_b = e_b m_b = \rho_{E,b} \tau_b \tag{10.5b}$$

$$P_b = p_b m_b = \rho_{P,b} \tau_b \tag{10.5c}$$

where τ_b and m_b are, respectively, the battery's volume and mass. Mass can be evaluated considering the energy content too, but Equation (10.5a) is more intuitive and based on the physical meaning of density, and thus it has been used. To not damage the component, a battery can never be fully discharged; state of charge (SoC) is defined to monitor its state. It is defined as the ratio between the energy still available at a certain time $E(t)$ and the total energy stored E_b:

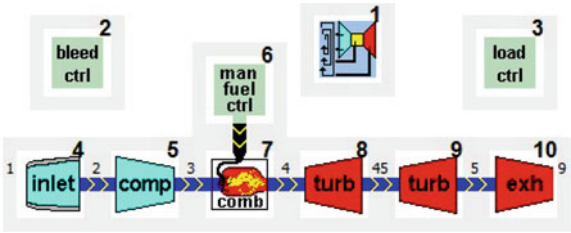

Fig. 10.3 Turboshaft scheme, as modeled in GSP (software developed at NLR)

$$SoC(t) = \frac{E(t)}{E_b} = 1 - \frac{E_c(t)}{E_b} \tag{10.6}$$

in which $E_c(t)$ is the energy consumed at time t. SoC lower limit generally depends on battery's type; for a Li-Ion, it is 20% (Tremblay and Dessaint 2009). This is a key aspect in an hybrid aircraft, as it will be explained in the following.

10.3.2 Gas Turbine Generator Model

The other energy source is the gas turbine generator, ensemble of a fuel burning engine and a converter device (to convert mechanical power into electrical power). Turboshaft is modeled outside the aircraft design process and it is not included into the sizing loop. Software used for modeling is GSP (Gas Turbine Simulation Program) developed at Netherlands Aerospace Research Center NLR (Visse and Broomhead 2000). The schema is shown in Figure 10.3. A single compressor has been used, meanwhile there are two turbines after the combustion chamber: high speed turbine, connected to compressor, and low speed turbine, where the power converter is mounted on. Model's outputs are the power and the power specific fuel consumption (PSFC), depending on the altitude and the Mach number. Once these curves are obtained, they are provided to the code and interpolated to get the value of interest for performance. Once the component specific power density is defined, the weight is computed as:

$$m_{gen} = \frac{P_{ts,des}}{p_{ts}} + \frac{\eta_g P_{ts,des}}{p_g} \tag{10.7}$$

where $P_{ts,des}$ is the power delivered at the design point, p the power density, η the efficiency, and the subscripts ts and g refer to turboshaft and generator, respectively.

10.3.3 Other Electric Components

Other electrical components (motor, inverter, and converter) just introduce a weight penalty m, that can be computed, knowing the maximum load power $P_{\max}$, as:

$$m = \frac{P_{\max}}{p} \tag{10.8}$$

with p being the specific power density (or power to mass ratio). Cables have to transport current from one device to another within the hybrid architecture, and their size is mainly determined by the maximum allowable current threshold and the transport voltage. Finally, ducted fans are sized starting from the evaluation of inner thermodynamic transformation, as shown in Sgueglia et al. (2018a). The condition of coupling between motors and fan (the torque is the same for both) is assured during the loop. Ducted fans introduce a penalty in aerodynamics, since they contribute to increase the wetted area, and thus the drag coefficient.

10.4 Description of the Fixed-Wing Aircraft Sizing Tool

The tool here used is called FAST (Fixed-wing Aircraft Sizing Tool), described in the work of Schmollgruber et al. (2017). It is an aircraft sizing code, fully developed in Python, based on the point mass approach to estimate the required fuel consumption for a given set of top level aircraft requirements (TLAR). It has been validated for a large range of configurations: large passenger turbojet (Schmollgruber et al. 2017, 2018), regional aircraft (Bohari et al. 2018), hybrid electric (Sgueglia et al. 2018a), and even Blended Wing Body (Sgueglia et al. 2018b). It considers key disciplines (aerodynamics, structure/weight, and propulsion) within a multidisciplinary design analysis and optimization framework. According to user's needing, only a simple MDA can be run, or all the optimization process. The general FAST's scheme, using the xDSM (eXtended Design Structure Matrix) standard (Lambe and Martins 2012), can be seen in Figure 10.4. The main workflow is identified by the black line. At the top level there is the loop controller (rounded block); then there is an inner loop, which represents the sizing process where disciplines are iteratively called until the convergence is reached. Note that analyses exchange information; data sharing is identified by the gray line. Aircraft is sized with respect to a set of design variables (geometrical, propulsive, or others) subject to a set of design constraints (certifications, airport constraints, and so on). The convergence is driven by mainly two conditions:

- structure's convergence. At each iteration, a new value of Maximum Take−Off Weight (MTOW) is estimated, when relative difference between two consecutive values is under the required tolerance, then structure has converged.

- batteries convergence. This condition only applies to hybrid electric aircraft, and requires that the SoC, at the end of flight's simulation, is equal to 0.20. With this condition it is assured that the trajectory is electrified as much as possible; in case is higher than 0.20 then it is still possible to use energy and the fuel consumption can be still reduced.

  To check the last condition, final battery's volume value is

$$\tau_b = \frac{E_c}{\left(1 - SoC_f\right) \rho_{E,b}}. \tag{10.9}$$

Equation (10.9) is deduced combining Equations (10.6) and (10.5b). Another check is also done to ensure that batteries' volume fits in cargo. Other design constraints are applied, but a full description of them is beyond the scope of this work.

Technological parameters mainly impact the mass breakdown analysis (where all the weights are computed), but their effects are not simply as simple as considering just mass penalties, because stronger connections between the disciplines. For example, considering the battery, specific energy density impacts the energy available; a reduction of this parameter reflects in two ways:

- keeping the mission's electrification constant, a weight divergence due to the increasing in batteries' volume,
- keeping the batteries' volume constant, a different mission's electrification, in which the fuel burning engine is widely used.

In both cases the energy consumption is higher, but a priori is not possible to say which case is the most conservative. Vice versa happens considering an increasing specific energy density. Others electrical components play a key role too: their efficiencies change the power available (see Equations (10.2) and (10.3)), which affects both the energy consumption (because the power and then the thrust available change) and the mass (because maximum power changes too). In conclusion, the technological effect is not as intuitive as anyone can think, and to understand their impact there is the needing to set up a MDAO, capable to handle the problem. The other relevant issue on technologies is linked to uncertainty: in the bibliography, there are different assumptions for the 2035 perspectives (see Brelje and Martins 2018; Sgueglia et al. 2018a; Friedrich and Robertson 2015; Hepperle 2012; Bradley and Droney 2015; Fraunhofer 2011; Belleville 2015; Cinar et al. 2017; Pornet et al. 2014; Anton 2017; Delhaye 2015). To evaluate the uncertainty effects, a sensitivity analysis is set up. The assumption that each component has the same mean value is done (that is, there is no fabrication error but each battery, motor, etc. are perfectly equal), and the exploration points are uniformly spaced. Under these hypotheses, an analysis is performed, to get the impact of technologies on some key parameters and to identify the most relevant ones. Two different approaches are used: one in which the geometry is totally fixed, and another one in which sizing loop on batteries is considered, underlining the importance of evaluating technologies in the integrated

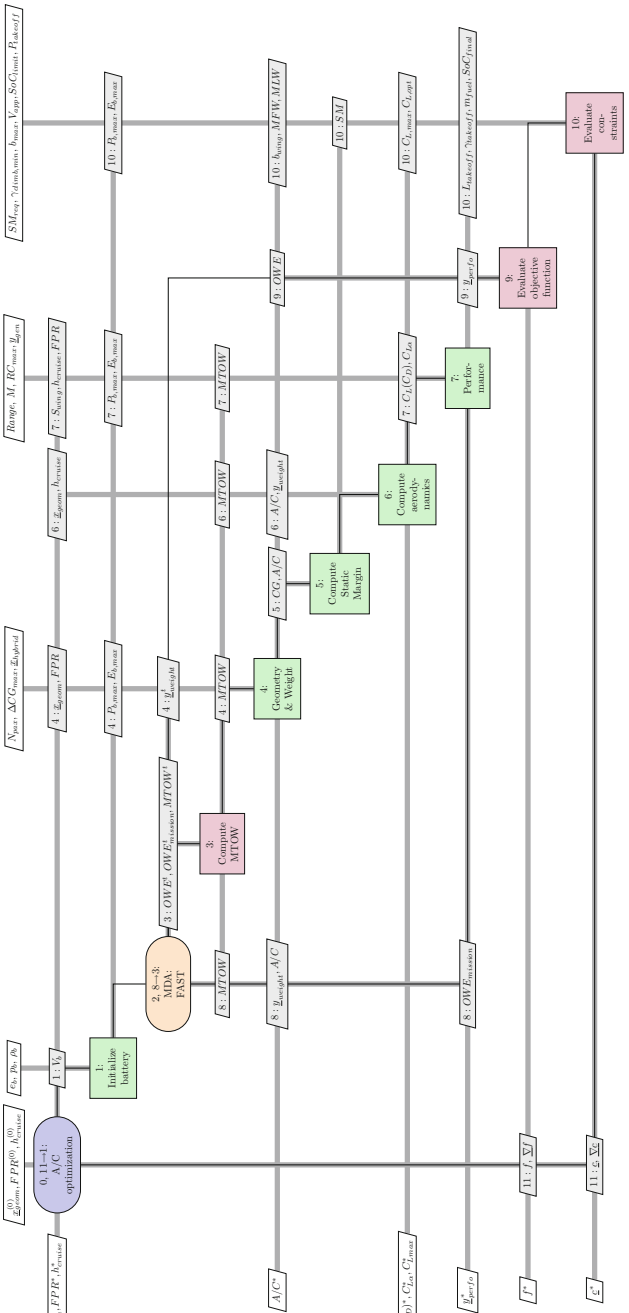

Fig. 10.4 FAST xDSM. Black lines represent the main workflow; thick gray lines represent the data flow, meanwhile green blocks indicate an analysis, gray and white block an input/output data

process, since an off-design analysis can be misleading. Before presenting the results, a brief review of the method used is presented in next section.

10.5 Global Sensitivity Analysis

10.5.1 Objective of the Global Sensitivity Analysis and Retained Methodology

As stand previously, one of the challenges in the design of a hybrid electric aircraft at horizon 2035 is to assess the future characteristics of the technological components. Indeed, a bibliography review reveals that the prediction of these characteristics presents a large dispersion. As an example, according to Hepperle (2012) the specific density energy e_b should be set to 350 W h kg^{-1}, whereas Bradley and Droney (2015) recommend to use a value of 750 W h kg^{-1}. The same kind of variations can be found for all the parameters relevant to the hybrid electric aircraft sizing, namely the density ρ_b, the battery efficiency η_b, the turboshaft power density p_{ts}, the generator power density p_g, the generator efficiency η_g, the electric motor power density p_{em}, the electric motor efficiency η_{em}, the inverter converter power density p_{ic}, the inverter converter efficiency η_{ic}, and the cooling system power density p_{cs}. To lighten the notations, these 11 parameters are concatenated into a vector denoted by $\mathbf{U} = \left\{e_b, \rho_b, \eta_b, p_{ts}, p_g, \eta_g, p_{em}, \eta_{em}, p_{ic}, \eta_{ic}, p_{cs}\right\}$. Note that in Table 10.1, battery's power density is missing, for what said in Section 10.3.1 it depends solely on battery's energy density. It is assumed that $p_b = 4e_b$, which is a compromise between energy stored and power delivered.

In order to evaluate the impact of the uncertainty affecting the parameters on the design of the aircraft, a global sensitivity analysis of the operating weight empty (OWE) and of the energy consumption (E_c) with respect to $\mathbf{U}$ is proposed in the next section. The first step of this sensitivity analysis consists in modeling the vector $\mathbf{U}$ with a suitable probabilistic model $\mathbf{U}$. According to the information found during the literature review, it is assumed that the random parameters are uniformly distributed between the minimal and the maximal values provided in the literature. Moreover, to the best of our knowledge, the correlation between those parameters has not been studied yet, as a consequence independent assumption is retained in the following. Table 10.1 gives the boundaries of the uniform distribution for each component of the vector $\mathbf{U}$ as well as the mean value μ and the coefficient of variation $\sigma^\star = \frac{\sigma}{\mu}$ (where σ stands for the standard deviation). Next section details the computation of Sobol sensitivity indices by Polynomial Chaos Expansion used in the present study.

Remark It should be noted that the proposed probabilistic model is designed to model the *large* uncertainties due to a lack of knowledge about the 2035 technology, in particular this model is not suited to model the *small* variations due to manufacturing process or inherent to the materials. Indeed, one can note that the same random variables are used for multiple similar components (as an example

it is assumed that the electric motor efficiency is the same for all motors). This assumption is obviously wrong if one deals with *small* manufacturing uncertainties (i.e., all manufactured electric motors efficiency are slightly different) but in our context it can be justified as the considered uncertainties are much more larger and represent the hypotheses on the future technologies.

10.5.2 Computation of Sobol Indices by Polynomial Chaos Expansion

This section recalls some basic features about the computation of Sobol sensitivity indices by Polynomial Chaos Expansion (PCE, see Chapter 3 on PCE and sensitivity analysis). Sobol sensitivity indices are variance based sensitivity measure that quantify how the variance of an input is responsible for the variance of the output. Their estimation can be achieved by Monte Carlo sampling (Sobol 1993), however an interesting approximation by PCE is proposed in Sudret (2008) that is very efficient in terms of numerical cost in the context of this study (low number of input variables and smooth mapping between inputs and outputs). This approach has been further improved in Blatman and Sudret (2010b) using sparse PCE and will be used in the following.

For the purpose of explanation, we introduce $\mathbf{U} = \left\{U^{(i)}\right\},\ i = 1, \ldots, d$ (where d is the number of input variables) a random vector modeling the input parameters of d independent components, $\mathscr{M}(\cdot)$ a numerical solver (FAST in this case) and $Y = \mathscr{M}(\mathbf{U})$ a scalar output. In the hypothesis in which Y is a second-order random variable, it can be shown that (Cameron and Martin 1947)

Table 10.1 Uniform probability distribution characteristics for random technological parameters used in HE aircraft sizing

		Min.	Max.	μ	$\sigma^\star$
e_b	[W h kg^{-1}]	350	750	550	0.21
ρ_b	[kg L^{-1}]	1.5	2	1.5	0.08
η_b		0.9	0.98	0.94	0.02
p_{ts}	[kW kg^{-1}]	5.5	8.5	7.0	0.12
p_g	[kW kg^{-1}]	12	15	13.5	0.06
η_g		0.85	0.98	0.915	0.04
p_{em}	[kW kg^{-1}]	8	12	10	0.11
η_{em}		0.95	0.99	0.97	0.01
p_{ic}	[kW kg^{-1}]	15	20	17.5	0.08
η_{ic}		0.9	0.99	0.945	0.03
p_{cs}	[kW kg^{-1}]	1.5	2.5	2	0.14

$$Y = \sum_{i=0}^{\infty} C_i \phi_i(\mathbf{U}) \tag{10.10}$$

where $\{\phi_i\}_{i\in\mathbb{N}}$ is a polynomial basis orthogonal with respect to the probability density function (PDF) of $\mathbf{U}$ (Legendre polynomials in case of uniform PDF) and C_i are unknown coefficients. Sparse PCE by least angle regression (LAR) proposed by Blatman and Sudret (2010a) consists of the construction of a sparse polynomial basis $\{\phi_i\}_{\alpha\in\mathscr{A}}$, where $\alpha = [\alpha_1, \ldots, \alpha_d]$ is a multi-index used to identify the polynomial acting with the power α_i on the variable $U^{(i)}$ and $\mathscr{A}$ is a set of index α. In practice, $\mathscr{A}$ is a subset of the set $\mathscr{B}$ which contains all the indices α up to a degree q, i.e. $card(\mathscr{B}) = \frac{(q+d)!}{q!d!}$. The objective of the sparse approach is to find an accurate polynomial basis $\{\phi_i\}_{\alpha\in\mathscr{A}}$ such as card($\mathscr{A}$) << card($\mathscr{B}$). This is achieved by LAR, i.e. unknown coefficients C_i are computed by iteratively solving a mean square problem and selecting, at each iteration, the most correlated polynomial with the residual (Blatman and Sudret 2010a). Finally, the following approximation is deduced:

$$Y \approx \hat{Y} = \sum_{\alpha\in\mathscr{A}} C_\alpha \phi_\alpha(\mathbf{U}). \tag{10.11}$$

It should be noticed that, in practice, identification of the unknown coefficients by LAR needs the evaluation of the model $\mathscr{M}(\cdot)$ on a given design of experiments (DoE) sampled from the input space. Due to the orthogonality of the polynomial basis $\{\phi_i\}_{\alpha\in\mathscr{A}}$ it is possible to write:

$$\begin{cases} \mathbb{E}[\hat{Y}] = C_0 \\ Var[\hat{Y}] = \sum_{\alpha\in\mathscr{A}} C_\alpha^2 \mathbb{E}[\phi_\alpha^2(\mathbf{U})] \end{cases} \tag{10.12}$$

where $\mathbb{E}[\hat{Y}]$ is the mean value and $Var[\hat{Y}]$ is the variance of the output variable $\hat{Y}$. It is shown in Sudret (2008) that PCE can be identified to the analysis of variance (ANOVA) decomposition, from which it is possible to show that the first-order sensitivity index of the variable $U^{(i)}$ is

$$\hat{S}_i = \frac{\sum_{\alpha\in L_i} C_\alpha^2 \mathbb{E}\left[\phi_\alpha^2(\mathbf{U})\right]}{Var[\hat{Y}]} \tag{10.13}$$

where $L_i = \left\{\alpha \in \mathscr{A} / \forall\, j \neq i \;\alpha_j = 0\right\}$; that is, only the polynomials acting exclusively on variable $U^{(i)}$ have been considered. The total sensitivity index can also be computed:

$$\hat{S}_{T_i} = \frac{\sum_{\alpha\in L_i^+} C_\alpha^2 \mathbb{E}\left[\phi_\alpha^2(\mathbf{U})\right]}{Var[\hat{Y}]} \tag{10.14}$$

where $L_i^+ = \{\alpha \in \mathscr{A}/\alpha_i \neq 0\}$; that is, all the polynomials acting on the variable $U^{(i)}$ have been considered (which means that all variance caused by its interaction, of any order, with any other input variables are included). Indices sum (first order or total) gives indication about the interaction between variables: if it is equal to one, then no interaction exists, i.e. polynomials of more than one variable in decomposition given by Equation (10.11) are meaningless. On the contrary, if the total indices sum is greater than one (i.e., the first-order indices sum is less than one), then the weight of interactions between input variables is not negligible in the total variance of the response and these interactions need to be investigated more precisely.

One can note that the accuracy of the sensitivity indices estimated thanks to PCE depends on the maximum degree q of the polynomials contains in the candidate basis $\mathscr{B}$ and on the DoE used to compute the unknown coefficients C_α in Equation (10.11). Inspired by Dubreuil et al. (2014), the following approach is set up in order to quantify the robustness of the results presented in Section 10.6. First the degree q is set to $q = 3$ leading to $\text{card}(\mathscr{B}) = 364$ (we recall that the number of uncertain parameters is $d = 11$). Second, the DoE size is set to 400. Over these 400 points, 350 are used for the computation of the unknown coefficients (points denoted as training set in the following), the remaining 50 points are used as validation set (computation of the relative mean square error). To assess the robustness of the indices with respect to the training set, a bootstrap approach (Efron 1979) is used, i.e. the training set and the validation set are randomly chosen, the unknown coefficients of the PCE are computed and the corresponding sensitivity indices are estimated. These computations are repeated B times leading to an estimation of the mean values and the coefficients of variation for each sensitivity index. In practice, B is set to 100 in this study.

10.6 Results

In this section, PCE is used to analyze the impact of technology uncertainties on the HE aircraft design. Table 10.2 reports the top level aircraft requirements (TLAR): the range has been chosen because it is the limit range in which the HE concept is still advantageous compared to a conventional aircraft. The number of passengers is the same of an Airbus A320 aircraft, 40 engines and 4 batteries are used. It should be noted that, since the model is linear, there is no difference in considering 1, 4, or more batteries, but the number is chosen only considering the cargo dimension constraints, in order to fit them in the available space.

The Sobol indices are computed considering key parameters: operating weight empty (OWE), to get the effect on structure's weight and energy consumption (E_c), to estimate impact on performances. The latter is a more significant parameter than the fuel consumption, since the aircraft is dual energy; considering the fuel

consumption, in fact, removes the batteries' contribution. DoE consists of 400 points, uniformly distributed according to the probabilistic model proposed in Table 10.1; a Latin Hypercube Sampling (LHS) is used for its generation.

In the next sections, two different sensitivity analyses are performed: in the first one, batteries' geometry is fixed and the sizing tool reaches a viable aircraft, in which structure's weight changes due to different technologies. The drawback of these runs is that the final state of charge is not 0.20, and then the points are not comparable, as described in Section 10.4. In the second case, instead, batteries' geometry is changing to always get $SoC_f = 0.20$ (see Equation (10.9)): in this case all the configurations have drawn all the possible electrical energy and points are at the same energetic level. The mission's electrification is the same for all the points. These analyses allow to underline the differences when technologies are studied in off-design condition and when they are directly integrated into the sizing process: the last is more interesting from a designer, since aircraft design problem is made up by different disciplines, coupled to each other.

Table 10.2 Top level aircraft requirements (TLAR) used to size the HE concept

Range	1200	NM
Mach number	0.7	
Passengers	150	
Number of engines	40	
Number of batteries	4	

Table 10.3 Mean first-order indices, together with their coefficient of variation, related to key parameters

	OWE		E_c		SoC_f	
	μ	σ^*	μ	σ^*	μ	σ^*
e_b	0.0774	0.0496	0.0681	0.2371	**0.7336**	0.0579
ρ_b	**0.5425**	0.0087	**0.2686**	0.0859	**0.2385**	0.1763
η_b	0.0344	0.0026	0.0149	0.8060	0.0014	8.739
p_{ts}	0.0902	0.0428	0.0391	0.3603	0.0016	8.033
p_g	0.0062	0.2931	0.0027	2.713	0	0*
η_g	0.0992	0.0036	0.0429	0.3468	0.0039	4.214
p_{em}	0.0594	0.0493	0.0258	0.5353	0.0013	9.179
η_{em}	0.0132	0.1603	**0.1088**	0.173	0.0015	9.920
p_{ic}	0.0236	0.1064	0.0100	1.054	0.0004	22.84
η_{ic}	0.0001	5.327	**0.3935**	0.0597	0.0004	26.50
p_{cs}	0.0482	0.0620	0.0215	0.6198	0.0011	12.70
Sum	0.9944		0.9961		0.9836	

Fixed battery case
The highest values are in bold

Table 10.4 Mean value and coefficient of variation of mean square error on training set for key parameters considered. Fixed battery case

	μ	σ^*
OWE	3.4×10^{-9}	8244
E_c	5.0×10^{-6}	172.3
SoC_f	3.4×10^{-4}	24.32

10.6.1 Sensitivity Analysis—Fixed Battery

The first presented analysis consists in keeping the battery fixed, MDA only enforces the convergence of all the masses to a viable aircraft. Even if the drawback of this approach is that points are not at the same final energy level, it allows at least to evaluate which are the parameters that impact SoC. Table 10.3 reports the first-order Sobol indices mean value, related to OWE, E_c, and also SoC_f, together with their coefficient of variation (estimated by 100 resamples as explained in Section 10.5.2). In case the mean value is zero, by convention σ^* is replaced by the standard deviation σ. An asterisk superscript identifies the cases in which the convention is applied (leading to $\sigma = 0$ in the present case). The main contribution to OWE is due to the battery density ρ_b, since it affects the battery's weight (see Equation (10.5a)) and represents the biggest percentage on structure's weight. Other contributions are distributed between the other parameters, which are in any case much less important. Battery's density is also the main parameter on E_c, but also efficiencies play a role: recalling Equations (10.2) and (10.3), they define the power delivered through the energy chain, and energy is directly related to power by time step. Note that efficiencies have also more importance than the power densities: mass penalties have a smaller contribution than the power level. Finally, SoC is mainly affected by battery's specific energy and density, as expected since by combining Equations (10.6) and (10.4a) it emerges that SoC is function of these two parameters (e_b and ρ_b). Another remarkable result is that coefficient of variation is very large when the effect is not relevant: when the Sobol index is very low, design of experiments strongly affects results. However, since the effect is negligible, this limitation does not create problems in final analysis. Finally, indices' sum is close to one: no interactions between variables are present.

To be sure about the validity of results, the mean square error (MSE) is computed on the training set. As done for the Sobol indices, the mean value and the coefficient of variation for the 100 repetitions are computed; values are reported in Table 10.4. The mean value μ is very small, meanwhile σ^* is several orders of magnitude bigger, as expected recalling its definition. However, the quantity $\mu(1 \pm \sigma^*)$, which represents the limits of variation of MSE, is still under the tolerance of 1%, so validity of results is ensured.

Main effects can also be visually identified, plotting a scatter of points, as done in Figures 10.5, 10.6, 10.7, and 10.8, which show the effects of technology parameters

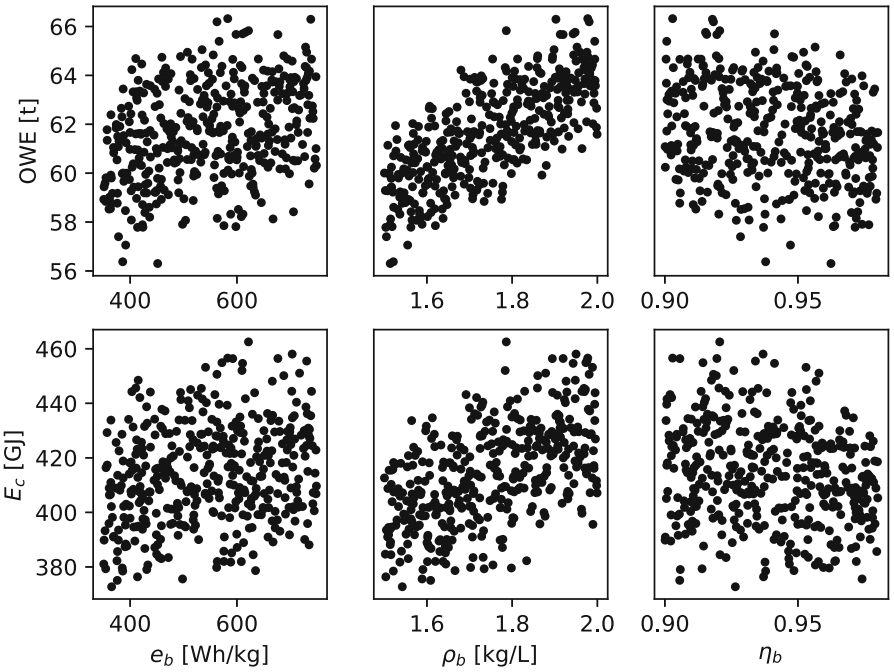

Fig. 10.5 Effects on OWE and energy consumption E_c of battery's technology parameters (energy density e_b, density ρ_b, and efficiency η_b). Fixed battery case

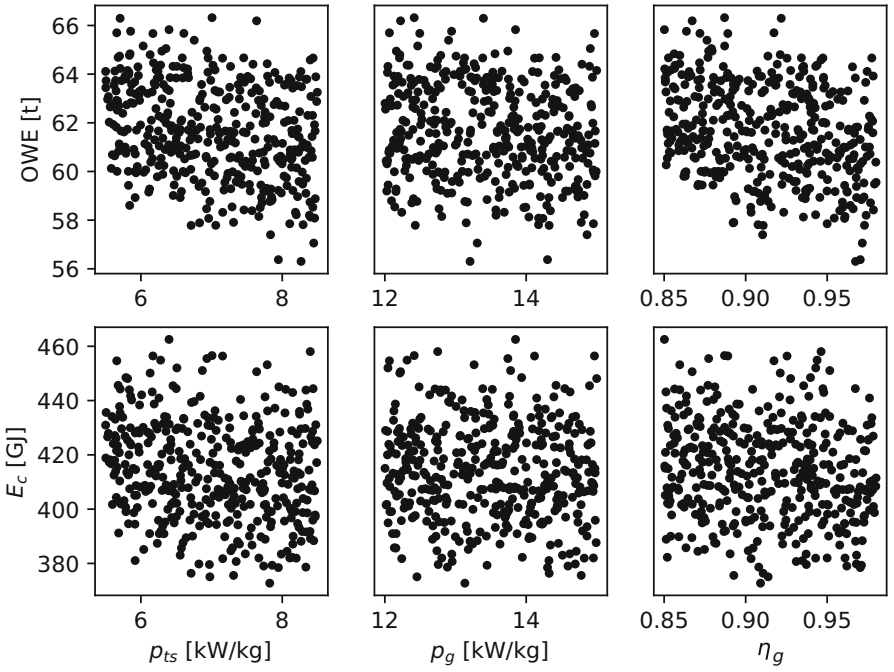

Fig. 10.6 Effects on OWE and energy consumption E_c of turbogenerator's technology parameters (turboshaft power density p_{ts}, generator power density p_g, and generator efficiency η_g). Fixed battery case

on the two key outputs (OWE and E_c). When there is a dominant effect, the points tend to align along a line, as, i.e. happens in the plot OWE-ρ_b; also more important is the parameter, more aligned are the points. It is also important to remark that the battery's energy density e_b does not have any importance on the structure and the energy consumption. At first glance this is in opposition with what explained in Section 10.3.1, but the reason lies in the fact that the geometry is fixed: the battery's volume is not changing, and thus a variation in e_b simply affects the energy stored, and as a consequence the final SoC. In the next paragraph, it is instead showed an analysis in which the SoC condition is implemented.

10.6.2 Sensitivity Analysis—Battery Resizing

This section presents the second analysis, in which the battery is resized to match the final SoC constraint. The same DoE as in the previous case is used. Together with OWE and E_c, also the battery volume τ_b is analyzed; Table 10.5 reports the values. It is immediately clear that in this case, due to the energy requirement, the battery's specific energy density e_b becomes the most relevant parameter; on the energy consumption there is still a contribution due to η_{ic} but it is smaller compared to previous analysis. What it is surprising is that the battery's density, that in an off-design analysis was the main player (see Table 10.3), now has impact 0 on OWE and E_c. The result can be explained combining Equation (10.4a) with Equations (10.9) and (10.5a), obtaining:

$$m_b = \frac{1}{e_b} \frac{E_c}{1 - SoC_f}. \tag{10.15}$$

Thus, the battery mass does not depend on its density. Still, it has a secondary contribution to battery's volume. Same remarks done in previous case on the coefficient of variations apply here too. Also, no interaction between variables is detected (first-order index sum almost equal to one).

Table 10.6 reports the data related to mean square error on training set: as already discussed for the previous case, the mean value is very small compared to the coefficient of variation, but even considering the total variation tolerance is under 1%, so also for this analysis results can be considered as valid.

This analysis shows that the HE aircraft is such a complex problem that it is not possible to evaluate the technologies in off-design conditions, as happened, i.e. for the mass reduction due to new materials, but they need to be evaluated

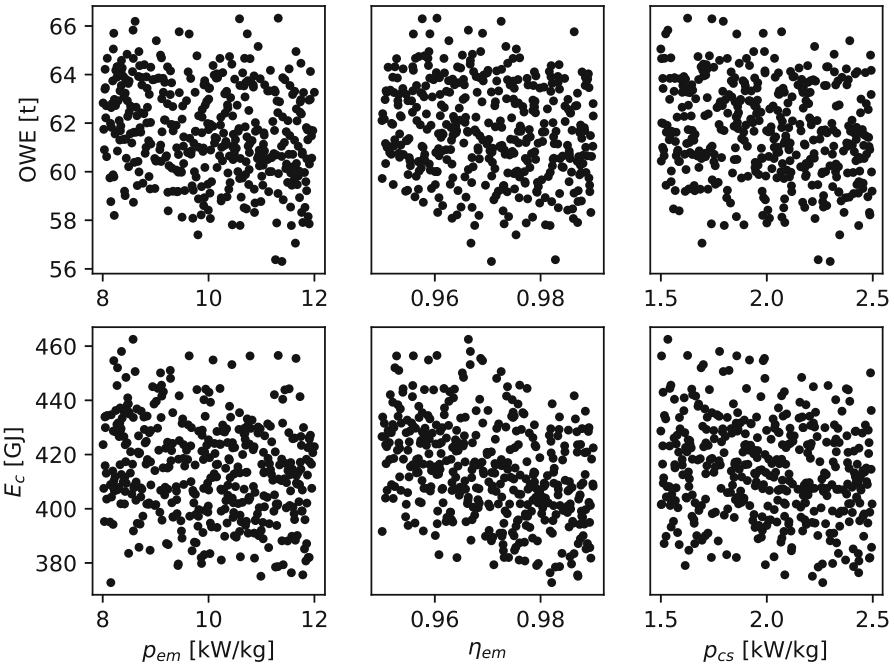

Fig. 10.7 Effects on OWE and energy consumption E_c of electric motor's and cooling system's technology parameters (EM power density p_{em}, EM efficiency η_{em}, cooling system power density p_{cs}). Fixed battery case

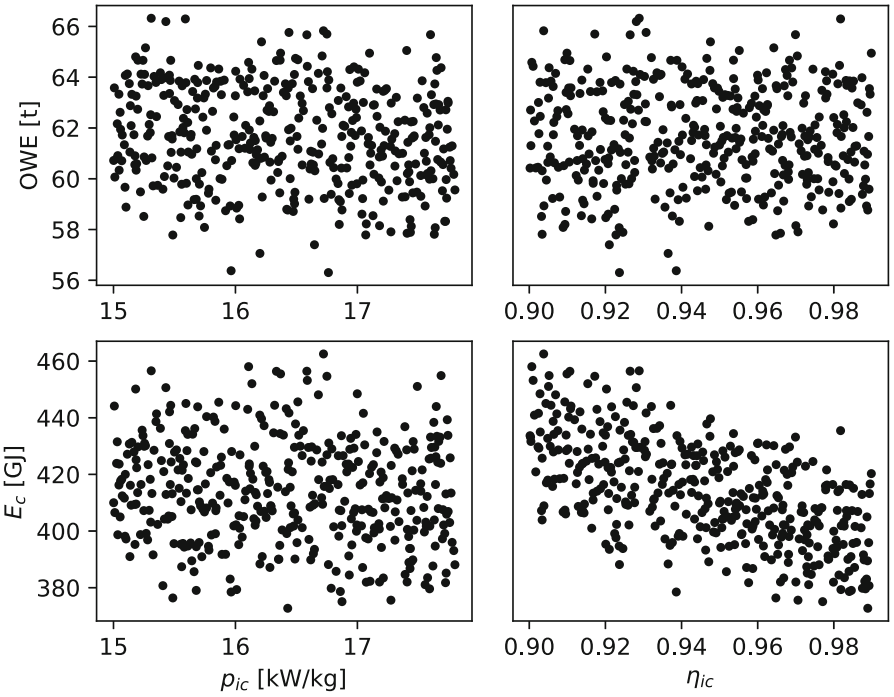

Fig. 10.8 Effects on OWE and energy consumption E_c of inverter's and converter's technology parameters (power density p_{ic} and efficiency η_{ic}). Fixed battery case

within the design process, otherwise results can be misleading. For completeness, in Figures 10.9, 10.10, 10.11, and 10.12 are shown the plot of each output with respect to each parameter.

To conclude, e_b is the most relevant player in the design process; every improvement done on the other parameters is non-sensitive as it. Also, it is to note that e_b is the parameter with the more incertitude, as shown in Table 10.1. Reducing the exploration range for this quantity, in the upcoming years, will be a main issue to have more accurate designs.

10.7 Summary

Aviation has found major interests in hybrid electric aircraft, to reduce its environmental impact within the next decades. Research has mainly focused in the problem of designing this type of unconventional aircraft, which is more complex than a conventional aircraft, due to the large couplings between the disciplines. Also, another issue arises, linked to technologies: in the literature, perspectives for electrical components' technological parameters in the next decades show a lot of uncertainties, that has to be taken into account. In the work here presented, a large passenger aircraft with distributed electric ducted fans, EIS2035, is first presented, together with the propulsive chain architecture and the models adopted for electrical components. This concept has been used to set up a sensitivity analysis, to estimate technologies' impact on the design process. The sizing tool considered is FAST, that is a multidisciplinary preliminary design aircraft sizing tool, which takes into

Table 10.5 Mean first-order indices, together with their coefficient of variation, related to key parameters

	OWE		E_c		τ_b	
	μ	σ^*	μ	σ^*	μ	σ^*
e_b	**0.9240**	0.0441	**0.7160**	0.0498	**0.8012**	0.0645
ρ_b	0	0^*	0	0^*	**0.1906**	0.2441
η_b	0.0119	0.0256	0.0090	2.932	0.0008	19.14
p_{ts}	0.0141	1.949	0.0107	1.996	0.0002	36.45
p_g	0.0005	20.35	0.0004	29.54	0	0^*
η_g	0.0183	1.467	0.0145	1.688	0	0^*
p_{em}	0.0089	2.822	0.0064	3.359	0.0003	33.74
η_{em}	0.0014	10.48	0.0440	0.8123	0	0^*
p_{ic}	0.0048	4.558	0.0041	4.644	0	0^*
η_{ic}	0	0^*	**0.1819**	0.2395	0	0^*
p_{cs}	0.0125	2.099	0.0095	2.388	0	0^*
Sum	0.9964		0.9964		0.9937	

Geometry optimized with respect to battery's volume to always get $SoC_f = 0.20$
The highest sensitivity index values are in bold

Table 10.6 Mean value and coefficient of variation of mean square error on training set for key parameters considered. Battery's resizing case

	μ	σ^*
OWE	5.7×10^{-5}	98.09
E_c	6.1×10^{-5}	91.53
τ_b	4.9×10^{-4}	31.62

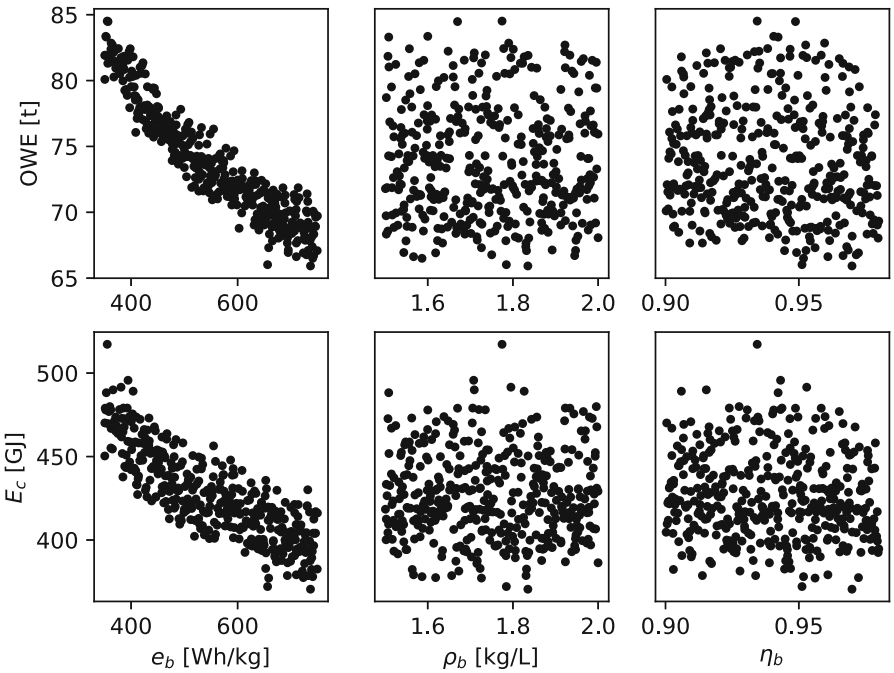

Fig. 10.9 Effects on OWE and energy consumption E_c of battery's technology parameters (energy density e_b, density ρ_b and efficiency η_b). Battery's resizing case

account all the key disciplines. It is described in Section 10.4. The method used for the sensitivity analysis is the Polynomial Chaos Expansion (PCE) method, described in Section 10.5. To evaluate the uncertainty, the assumption that each component has the same mean value and variance (that is, there are no fabrication errors) is done. The design space exploration has been built considering a lot of previous works for the chosen technological horizon. Two different problems have been studied: in the first one, technologies only act on masses, but the geometry is kept fixed, meanwhile in the second approach battery's volume is iteratively changed to always drawn all the allowable energy from it, and have all the points at the same energetic level. A comparison between the results of these two problems shows that it is not possible

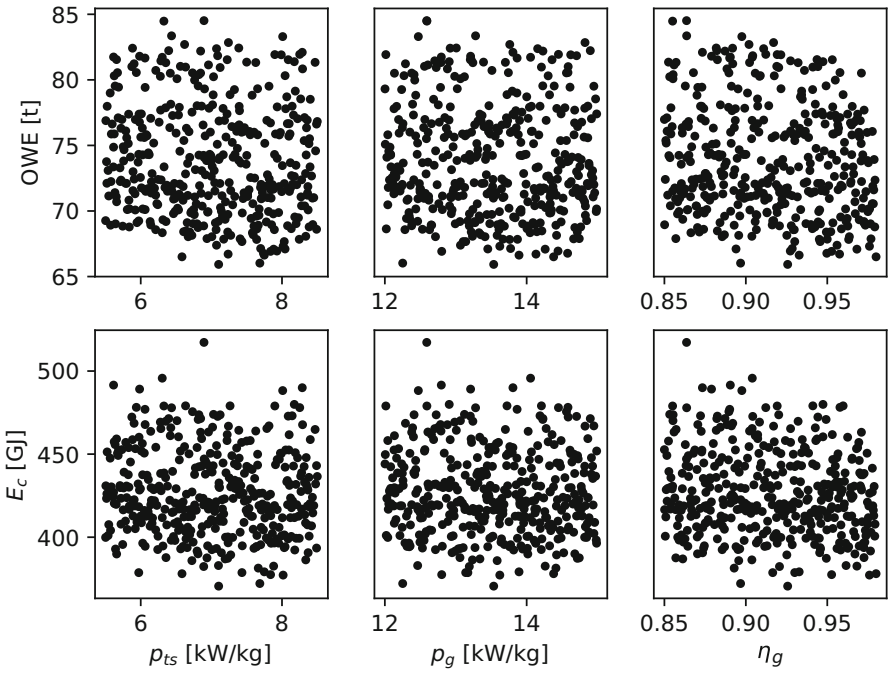

Fig. 10.10 Effects on OWE and energy consumption E_c of turbogenerator's technology parameters (turboshaft power density p_{ts}, generator power density p_g, and generator efficiency η_g). Battery's resizing case

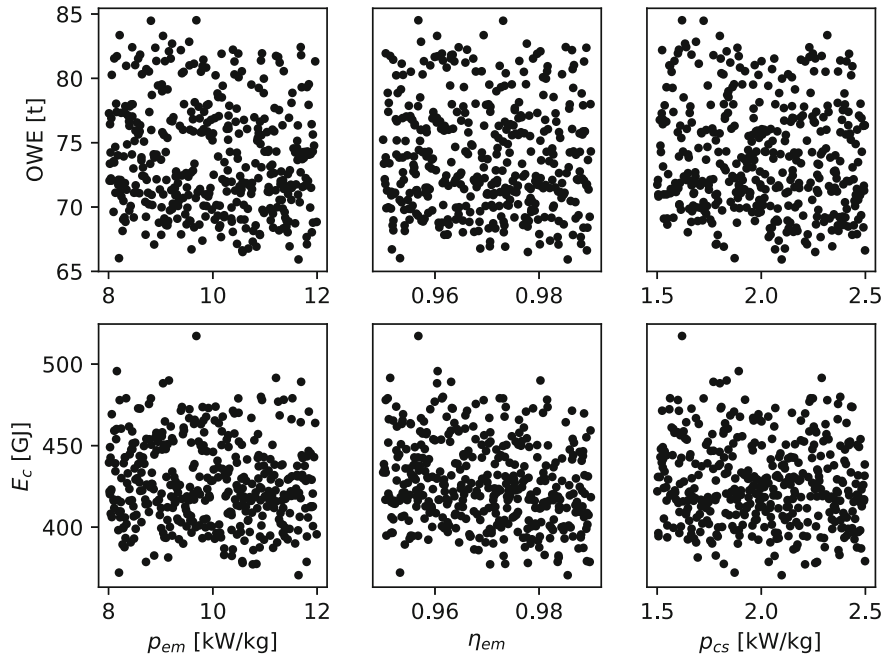

Fig. 10.11 Effects on OWE and energy consumption E_c of electric motor's and cooling system's technology parameters (EM power density p_{em}, EM efficiency η_{em}, cooling system power density p_{cs}). Battery's resizing case

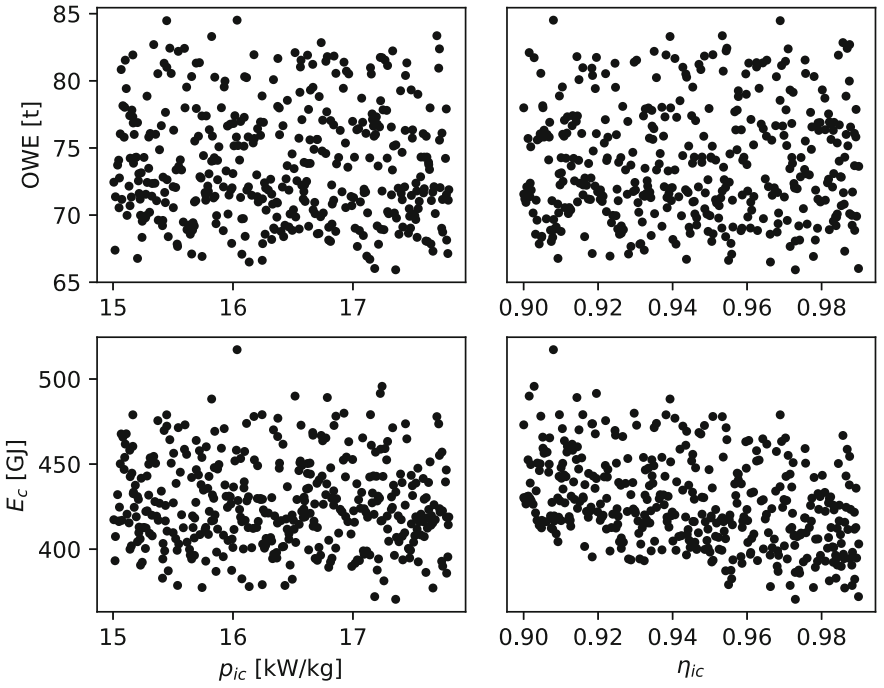

Fig. 10.12 Effects on OWE and energy consumption E_c of inverter's and converter's technology parameters (power density p_{ic} and efficiency η_{ic}). Battery's resizing case

to consider technologies out of the resizing loop (in off-design condition), since results can be misleading: from the first analysis, in fact, it emerges that the battery density is the most important parameter to focus on, but when batteries are resized the impact of this parameter is zero, being the specific energy density the driven parameter. This is also a simplification in which just one design variable is changed and one constraint is used: in this case there is an analytic solution to the problem, but aircraft is subject to multiple constraints (certification, airport limits, and so on) and in general all geometries' parameters are included as design variables. In any case it shows how complex it is to handle the problem of unconventional aircraft, giving reasonable results. Another conclusion is that design is mainly affected by the battery's specific energy density: on this parameter, in fact, there is the major uncertainty. For the upcoming years main focus should be to reduce uncertainty of this variable, otherwise any innovation in other electrical components will be useless since the sizing will always be affected by 90% from the batteries' design.

Acknowledgements The authors would like to thank Peter Schmollgruber (ONERA/DTIS) for his contribution in the developing of the tool FAST.

References

Anton, F. (2017). High-output motor technology for hybrid-electric aircraft. Cologne, Germany. eAircraft Electric & Hybrid Aerospace Technology Symposium.

Belleville, M. (2015). Simple hybrid propulsion model for hybrid aircraft design space exploration. pages 1–4, Toulouse, France. MEA-More Electric Aircraft conference.

Blatman, G. and Sudret, B. (2010a). Adaptive sparse polynomial chaos expansion based on least angle regression. *Journal of Computational Physics*, 230 (6):2345–2367.

Blatman, G. and Sudret, B. (2010b). Efficient computational of global sensitivity indices using sparse polynomial chaos expansions. *Reliability Engineering & System Safety*, 95 (11):1216–1229.

Bohari, B., Borlon, A., Mendoza Santos, P, B., Sgueglia, A., Benard, E., Bronz, M., and Defoort, S. (2018). Conceptual design of distributed propellers aircraft: Non-linear aerodynamic model verification of propeller-wing interaction in high-lift configuration. In *AIAA SciTech Forum, Kissimmee, FL, USA*.

Bradley, M. K. and Droney, C. K. (2015). Subsonic ultra green aircraft research: Phase II-volume II-hybrid electric design exploration. In *NASA report NASA/CR-2015-218704/Volume II*.

Brelje, B. J. and Martins, J. R. R. A. (2018). Electric, hybrid, and turboelectric fixed-wing aircraft: A review of concepts, models, and design approaches. *Progress in Aerospace Sciences*.

Cameron, R. H. and Martin, W. T. (1947). The orthogonal development of non-linear functionals in series of Fourier-Hermite functionals. *Annals of Mathematics*, 48(2):385–392.

Cinar, G., Mavris, D. N., Emeneth, M., Schneegans, A., Riediger, C., Fefermann, Y., and Isikveren, A. (2017). Development of a parametric power generation and distribution subsystem models at conceptual aircraft design stage. In *55th AIAA Aerospace Sciences Meeting, Grapevine, TX, USA*.

Collier, F. and Wahls, R. (2016). ARMD Strategic Thrust 3: Ultra-efficient Commercial Vehicles Subsonic Transport. In *Aeronautics R&T Roundtable, Washington, DC, USA*.

Delhaye, J. (2015). Electrical technologies for aviation of the future. In *Hybrid Electric Propulsion - Europe-Japan Symposium, Tokyo Japan*.

Dubreuil, S., Bervellier, M., Petitjean, F., and Salaün, M. (2014). Construction of bootstrap confidence intervals on sensitivity indices computed by polynomial chaos expansion. *Reliability Engineering & System Safety*, 121 (Supplement C):263–275.

Efron, B. (1979). Bootstrap methods: Another look at the jackknife. *The Annals of Statistics*, 7(1):1–26.

Fraunhofer (2011). Technology roadmap energy storage for electric mobility 2030.

Friedrich, C. and Robertson, P. (2015). Hybrid-electric propulsion for aircraft. *Journal of Aircraft*, 52(11):176–189.

Hepperle, M. (2012). Electric flight - potential and limitations. Braunschweig. Technical report, NATO.

Kirner, R. (2015). *An Investigation into the Benefits of Distributed Propulsion on Advanced Aircraft Configurations*. PhD thesis, Cranfield University.

Lambe, A. B. and Martins, J. R. R. A. (2012). Extensions to the design structure matrix for the description of multidisciplinary design analysis and optimization processes. *Structural and Multidisciplinary Design Optimization*, 46 (2):273–284.

Liebeck, R. H. (2004). Design of the blended wing-body subsonic transport. *Journal of Aircraft*, 41(1):10–25.

Lowry, J. and Larminie, J. (2012). *Electric Vehicle Technology Explained*. John Wiley & Sons, 2 edition.

Pornet, C., Seitz, A., Isikveren, A. T., and Hornung, M. (2014). Methodology for sizing and performance assessment of hybrid energy aircraft. *Journal of Aircraft*, 52(1):341–352.

Schmollgruber, P., Bartoli, N., Bedouet, J., Benard, E., and Gourinat, Y. (2018). Improvement of the aircraft design process for air traffic management evaluations. In *AIAA SciTech Forum, Kissimmee, FL, USA*.

Schmollgruber, P., Bedouet, J., Sgueglia, A., Defoort, S., Lafage, R., Bartoli, N., Gourinat, Y., and Benard, E. (2017). Use of a certification constraints module for aircraft design activities. In *AIAA Aviation Forum, Denver, CO, USA*.

Seresinhe, R. and Lawson, C. (2014). Electrical load-sizing methodology to aid conceptual and preliminary design of large commercial aircraft. *Journal of Aerospace Engineering*, 229 (3):445–466.

Sgueglia, A., Schmollgruber, P., Bartoli, N., Atinault, O., Benard, N., and Morlier, J. (2018a). Exploration and sizing of a large passenger aircraft with distributed electric ducted fans. In *AIAA SciTech Forum, Kissimmee, FL, USA*.

Sgueglia, A., Schmollgruber, P., Benard, E., Bartoli, N., and Morlier, J. (2018b). Preliminary sizing of a medium range blended wing-body using a multidisciplinary design analysis approach. volume 233. MATEC Web of Conferences.

Sobol, I. M. (1993). Sensitivity estimated for nonlinear mathematical models. *Mathematical modelling and computational experiments*, 1(4):407–414.

Sudret, B. (2008). Global sensitivity analysis using polynomial chaos expansions. *Reliability Engineering & System Safety*, 93 (7):964–979.

Tremblay, O. and Dessaint, L.-A. (2009). Experimental validation of a battery dynamic model for EV applications. *World Electric Vehicle Journal*, 3:289–298.

Visse, W. P. J. and Broomhead, M. J. (2000). GSP: A generic object-oriented gas turbine simulation environment. NLR, NLR-TP-2000-267.